university of groningen

faculty of science and engineering

Self-Assembly and Optical Spectroscopy of J-type Organic Nanostructures

Gayeon Kim

university of groningen / faculty of science and engineering

University of Groningen

SELF-ASSEMBLY and OPTICAL SPECTROSCOPY of J-type Organic Nanostructures

Bachelor's Thesis

To fulfill the requirements for the degree of
Bachelor of Physics
at University of Groningen under the supervision of
Ioannis Touloupas (phd researcher, University of Groningen)
and
Prof. R. Hildner (Zernike Institute for Advanced Materials, University of Groningen)
and
Prof. T. L. C. Jansen (Zernike Institute for Advanced Materials, University of Groningen)

Gayeon Kim(S3541223)

December 12, 2021

Contents

Acknowledgments

I would like to thank the following people. First of all, my sincere thanks to Ioannis Touloupas who supervised my whole research project and also provided me sound education and truthful, positive support. And professor Richard accepted me in this scientifically inspiring team and always guided me with the best feedbacks and education as well. Also, Foppe never hesitated to help me with the experiments. I feel very grateful for all the people who helped me during this project.

Abstract

This research is about investigating properties of self-assembly in organic nanostructure. We compare UV/VIS and absorption spectra of the CBT (carbonyl-bridged triarylamine) monomer, by dissolving in THF (tetrahydrofuran), and the J-aggregated nanofibres, in MCH (methylcyclohexane). The effects of concentration on the aggregation process were studied. Then, heat treatments on the assemblies were applied for 30, 60, 120 minutes to optimize the preparation of nanofibers and assess the effect by comparing spectral features. Though no change in the absorption spectrum was observed, the fluorescence increased in aggregated solution after 120 minutes of heat treatment. Lastly, the fluorescence decay lifetime was measured with a streak camera, and the delocalization length of aggregate were computed. The delocalization length was found in the range from 13 to 40 monomers at room temperature.

1 Introduction

Nature already knows how to convert light into usable chemical energy. Chlorophyll absorbs light energy and transfers the energy to the plant's photosystem [1]. Photosynthesis has critical biological importance because it is required for practically all lives on Earth. Plants, algae, and bacteria use photosynthesis to generate chemical energy [2]. Artificial light -harvesting systems were inspired by this mechanism. Solar cell has been actively invented using the photovoltaic effect. Solar cells convert light energy into electricity, and increasing efficiency is a critical task for the future sustainable energy industry. The current studies show that the conversion efficiency can be maximized to around 14 to 22 percent for commercial photovoltaics [3] and 46 percent with a silicon wafer for solar cell made by Fraunhofer ISE [4]. Polymer solar cells occupies the majority of organic photovoltaic cells in the market [5]. Simple organic PV device uses a planar heterojunction. A layer of organic material that is either an electron donor or an electron acceptor lies between the electrodes. Excitons created in the active layer diffuse before separating, with each hole and electron diffusing to its own collecting electrode. Because excitons in conventional organic semiconductors have diffusion lengths of just 3–10 nm, planar cells must be thin, yet thin cells absorb light less well. [6].

But to the next step, supramolecular assemblies is one of the promising options that could be used for higher efficient exciton transport [7]. Main purpose is to improve to convert the solar energy in the cell or to the p/n hetero junction interface. In this case, minimizing energy loss is the task and researching aggregates might be helpful in nanoscale. By researching monomer and J-type aggregate molecule, the reason could be clear of why some characteristics of aggregate are critical in delivering solar energy with better energy conversion. It is promising to try out new aggregated materials to invent a new junction combination since every molecule structure has a different electronic structure, and that is connected to how the self-assembly performs as an energy carrier in the device.

The material used in this research project is CBT (carbonyl-bridged triarylamine). This material was used many times in other cases for recent studies about aggregates. The reason for using this material is that it has a triangular shape, and each molecule unit (monomer) can be stacked up based on π stacking. The electrons in the π orbital of a molecule interact with other electrons of other molecules next to each other, and they are linked together to form a long fiber. When the monomers are grouped, they have a certain basic unit number of monomers as one aggregate. This project is a fundamental research to test out optical properties of J-aggregate.

1.1 Research Questions

This paper is mainly focused on these research questions:

Q1. Identify effects of J-aggregation by comparing CBT mixed in two solvents under three different concentrations

Q2. Whether and how aggregation changes after exposure to specific temperature

Q3. Lifetime measurement and calculating delocalization of exciton in aggregate

1.2 Thesis Outline

The purpose of fundamental research is to determine if or how some factors can affect fluorescence or aggregation. From understanding theories and computational methods, the results will be analyzed so as to lead to a conclusion in terms of properties which will be discussed in the following sections. As preliminary step, the first set of experiments is to determine the characteristics of J-aggregates by applying theories and checking them in practice. Optimization of temperature resistance of this material will be the next task in the project. This optimization can be done by exposing the dissolved sample at a sufficiently high temperature at different time periods. Under different exposure times, the conclusion may be made if heat influences aggregation. It is also crucial to analyze the fluorescence decay and the delocalization in the exciton because these properties are directly related to the fluorescence rate compared to the given power and the repetition rate. So, the delocalization length of exciton can be calculated throughout the last phase.

2 Theory

2.1 Molecular spectroscopy

A material is composed of a great number of molecules. One atom has energy levels, and the energy level structure gets combined when many atoms form a molecule. By exciting a molecule, the absorption and emission spectrum give analysis about the energy profile. The energy profile between electronic and vibrational states provides information about the molecular structure [8].
First, an absorption spectrum can be achieved by stimulating an electron in the ground state to excited states above and this spectroscopy will be elaborated in section 2.1.1. Later, with the use of the absorption spectrum, the study will move on to emission spectroscopy. Transitions, such as rotational and translational energies, are not inspected in the analysis since they are not captured by the spectrophotometer. Interpretation of fluorescence and non-radiative emission will be discussed in section 2.1.2.

2.1.1 Absorption spectroscopy

Absorption spectroscopy is an analytical technique used to determine the molecular structure of the material. A light beam covering a certain wavelength range is shot onto the molecules, and some electrons are excited by the light when absorbing the light energy. The molecules are excited to multiple excited states from the ground state. The wavelength of absorbed light depends on the type of molecule and the energy gap in the energy levels ($E = \frac{hc}{\lambda}$) [8]. The transition probability depends linearly on the intensity of the incident light. That is the probability to absorb the light becomes high too. The probability of having corresponding energy represents the intensity of absorption at a specific wavelength, and the probability of the electron absorbing that certain energy follows the unnormalized Gaussian distribution. If electrons moving to other energy levels in the molecule absorb light at different wavelengths, then all the following gaussians are summed up on a graph resulting in the absorption spectrum of the molecule [9]. The Gaussian distribution equation is written as:

$$f(x) = \frac{I}{w\sqrt{2\pi}} e^{-\frac{1}{2}(\frac{x-E}{w})^2} \tag{1}$$

where f(x) is the probability density function. Coefficient 'I' describes the intensity of peak, this value contributes to normalization. Coefficient 'E' is the expectation value that indicates the photon energy of absorption or emissions, where it indicates highest intensity. This gives a guidance for picking wavelengths either excitation energy for fluorescence experiments. Coefficient 'w' means the linewidth, and more extensive c leads to having a wider peak. The width will tell how well the molecules are aggregated.
In terms of absorbance ($A(\lambda)$),

$$A(\lambda) = \sum_{i}^{\infty} f_i(\lambda) \tag{2}$$

The absorbance is determined by the concentration of molecules according to the Beer-Lambert law, which is explained at section 2.3.

2.1.2 Emission spectroscopy

The molecules in the excited states lose energy by various ways and tend to descend to a state of lower energy levels. Spontaneous emission is a phenomenon, which the transition to a lower state happens with no extra input. The electron in the excited state spontaneously loses vibrational energy which is small compared to the electronic transition energy, and it can reach the lowest vibrational state of the excited electronic state in between 10^{-14}s and 10^{-11}s. This loss of vibrational energy is non-radiative [10].

Fluorescence is a radiative process that shows transitions from excited states to the ground state. This happens in between 10^{-9}s and 10^{-7}s [10]. The intensity of emission light depends on the absorbance in the wavelength by the excitation wavelength. The numbers starting from 0 in fig [1b] are the vibrational state numbers in different excited states. (0,0) is the notation for transition between the lowest vibrational state (0) of the ground state and the lowest vibrational state (0) of the first excited state.

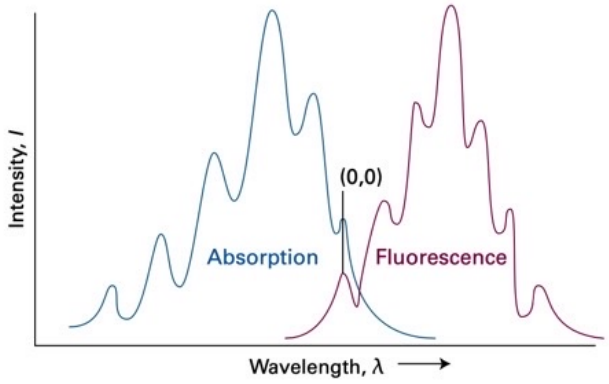

(a) Absorption and emission spectrum

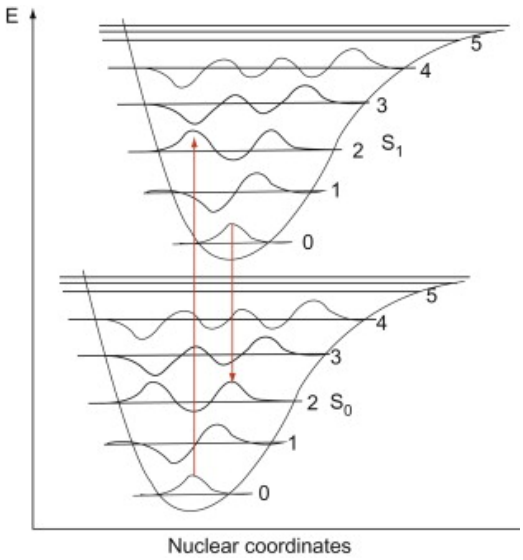

(b) Electronic transition from the ground state (S_0) to the first excited state (S_1) and vibrational transitions

Figure 1: Energy profile[8] of molecular structure and transition scheme

The excited molecule collides with the surrounding molecules [8]. When it emits non-radiative energy to the near molecules, its energy steps down to the lowest vibrational level of the excited electronic state. However, the surrounding molecules cannot always absorb the higher energy difference required to drop the molecule to its ground electronic state. As a result, the excited electronic state

takes time to perform spontaneous emission and radiate the remaining surplus energy. Franck Condon principle states that when the vertical energy transition occurs, the amplitude overlap of wavefunctions in different electronic states represents how the absorption or fluorescence spectrum is formed. According to the Franck Condon principle, the fluorescence spectrum looks mirrored perfectly to the absorption spectrum with respect to (0,0) transition. However, the axis of the emission spectrum in the actual experiments is expected to be slightly shifted toward the longer wavelengths side. The reason why the fluorescence spectrum is not a mirror shape is because of the interaction between molecules in the solution.

2.2 Types of molecular aggregates

2.2.1 Monomer

A monomer is approximated by a two-level system that is excited from the ground state to the first excited state without considering vibrational levels [7]. As a monomer system, a CBT core (carbonyl-bridged triarylamine)(fig [2]) was used in the experiment as an analyte and the solution was created by dissolving the CBT powder in solvent called Tetrahydrofuran (THF). The CBT core can be stacked up into self-assemblies by forming a Van der Waal interactions. So far, self-assembly enables long range transport which is up to 4μm [11].

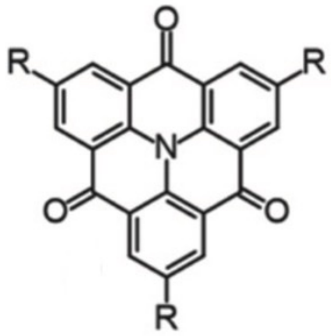

Figure 2: CBT molecular structure[11], R= n-octyl (C8H16)

For a mathematical analysis, an assumption begins with that each monomer unit does not interact with each other. It is also assumed that the monomers have no electronic interactions between the ground state and the excited state. So, the Hamiltonian about N sets of monomers is firstly given in the equation (3)[12].

$$H_0 = \sum_{n=1}^{N} E_0 |n\rangle\langle n| \tag{3}$$

where $|n\rangle$ is a wavefunction of the monomer 'n' in the excited state, E_0 is the eigenvalue and means the energy gap between the ground state and the first excited state. All the other monomers from 1 to N except for 'n' are in the ground state. All the monomer systems have the same excitation energy E_0.

2.2.2 H-aggregates

When monomers receive external force, those excited monomers create molecular excitons. The excitons are from the electronic coupling among the monomers [7].
In the aggregates, the electronic coupling , which is an involved interaction, is represented as V_{nm}.

$$V_{nm} = \frac{\mu_n \mu_m}{R_{nm}^6}(cos\alpha_{nm} - 3cos\beta_n cos\beta_m) = \frac{\mu_n \mu_m}{R_{nm}^6}\kappa \tag{4}$$

where $|\mu_{n(m)}|$ is the magnitude of the transition-dipole moment of monomer n or m, R_{nm} is the distance between the monomer n and m, and α_{nm}, β_n, and β_m are the angles as shown in fig [3a]. κ is the orientation factor. When the monomers are stacked up co-facially aligned, they form H aggregate. The direction of transition dipole moment (μ) is parallel to each other. In this case, κ is positive, as well as V_{nm}. Then from the monomer's Hamiltonian, the electronic coupling is simply added.

$$H = \sum_{n=1}^{N} E_0 |n\rangle\langle n| + \frac{1}{2}\sum_{n=1}^{N}\sum_{n\neq m} V_{nm}|n\rangle\langle m| \tag{5}$$

The nearest-neighbor approximation is that like in a linear chain which is composed of equally distanced monomers (symmetric aggregate), the monomers have the same electronic coupling V. So, the solution for the energy is:

$$E(k) = \langle k|H|k\rangle = E_0 + \frac{1}{2}\sum_{n=1}^{N}\sum_{n\neq m} V_{nm} e^{i2\pi k\frac{n-m}{N}} = E_0 + 2V_0 cos\frac{2\pi k}{n} \tag{6}$$

If N is even, k covers from 0 to $1, 2$, to $N-1$, which is equal to using the more symmetric boundaries $N/2 \leq k \leq N/2$ and $(N-1)/2 \leq k \leq (N-1)/2$ if N is odd. The exponential factor's magnitude is always 1. The exciton states are determined by adding the wavefunctions of the initial localized states while considering relevant phase relations. Then, the linear combinations of the exciton states of the aggregate becomes:

$$|k\rangle = \frac{1}{\sqrt{N}}\sum_{n=1}^{N} e^{i2\pi k\frac{n}{N}}|n\rangle \tag{7}$$

that means the probability to find an excitation at monomer n is $\frac{1}{N}$.
From each monomer, transition dipole moments interfere. In the $k = 0$ state, they interfere constructively and the transitions among aggregates are active so it becomes a bright state which is optically accessible. However, in the $k = N/2$ state, the moments interfere destructively and forms a dark state (optically inaccessible) since the transition to $k = N/2$ state is forbidden. In the equation $E(k)$, the energy has maximum at $E_0 + 2V_0$ and minimum at $E_0 - 2V_0$. For H-aggregates, the direction of transition of dipole moment (μ) of the monomers is parallel to each other. In this case, V_{nm} is bigger than 0 and excitation after absorption is stretched to the top of the bandwidth as seen in the fig[3a]. H-aggregate can be regarded completely non-emissive because the energy is higher in $k = 0$ having

$E = E_0 + 2V_0$ and lower energy in $k = N/2$ having $E = E_0 - 2V_0$. The relaxation process from $k = 0$ to $k = N/2$ happens faster than the decay into the ground state, and the transition from the lowest exciton state to the ground state is dipole-forbidden. So, the absorption spectrum is blue shifted than that of monomers.

2.2.3 J-aggregates

On the other hand, if the monomers form structures with dipole moments in a head-to-tail arrangement, then J-aggregates are created where the dipole-dipole interaction (V_{nm}) is negative. So unlike H-aggregate, when k= 0 in J-aggregate, the absorption to the electronic excited state reaches to the bottom of the energy band $E_0 + 2V_0$. This energy state is lower than the eigenvalue of the monomers. Consequently, the exciton can stay in the low and stable energy state, and there comes only radiative emission (vertical transition), no relaxation like H-aggregate. The radiative decay occurs faster by having a funneled energy than the decay of the monomers or H-aggregate. In fig [3], the arrows represent the optically accessible states at the bottom of J-aggregate's exciton bands. The transition with the thick arrow is optically allowed so the absorption is enhanced in certain energy gap. Therefore, J-aggregate has a sharp intense absorption peak in the spectrum and it is red-shifted compared to the monomer spectrum.
In the experiment, J-aggregates was only used for this research and was made by forming self assembly of the CBT molecule in methylcyclohexane (MCH).

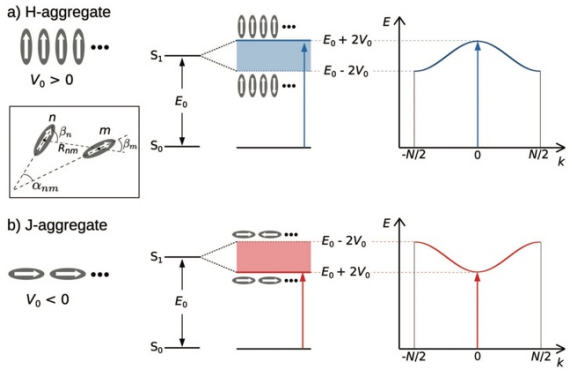

(a) H-aggregates and J-aggregates energy profile[12]

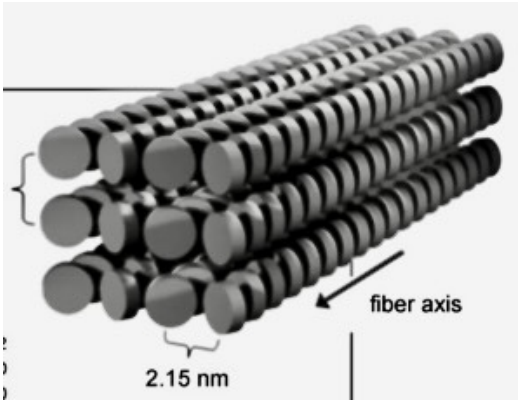

(b) Slip stacked J-aggregate[11]

Figure 3: H and J aggregates

2.3 Beer Lambert and cross section

The relationship between absorption and concentration of the sample is explained by equation [8]. This law states that the absorbance is proportional to the concentration, the length and absorptivity of the material.[13][8].

$$A = \varepsilon \cdot l \cdot c \tag{8}$$

where A is the measured absorbance, ε is the molar absorptivity of the attenuating species [$M^{-1}cm^{-1}$], l is the optical path length [cm], and c is the determined concentration of the species [M/mL]. The optical path length is the length of the cuvettes in the experiments, which were either 1cm or 0.1cm. During the experiment, the concentration of the solvents was varied as 0.25[mg/mL], 0.025[mg/mL] and 0.0025[mg/mL] depending on the experiments and according to the Beer Lambert law, it is expected that the high concentrated solvent in thick cuvette has the highest absorbance.

$$A = log(\frac{I_0}{I}) \tag{9}$$

When the absorbance A is 0.5 in 1cm thickness cuvette, for instance, the intensity at the center of the cuvette becomes only 0.316 of the intensity when the ray first enters the surface. The optical length in this law accounts for the decreasing light with the same liquid, but it could yield different absorbance by changing the concentration of the sample as well.
The concentration used in the Beer-Lambert law is molar concentration and it needs to be converted from mass concentration.

$$c_m[mg/mL] = c[mol/cm^3]m_m[mg/mol] \tag{10}$$

where c_m is the mass concentration, and c is the molar concentration, m_m is the molar mass. The molar mass for the used molecule is 828260[mg/mol] . By dividing the concentration by the molar mass, the extracted molar concentration is needed in order to find the cross section.

$$\sigma(\lambda)[cm^2] = \varepsilon/N_a = \frac{A(\lambda)}{N_a \cdot c \cdot l} \tag{11}$$

where N_a is the Avogadro number ($6.022 * 10^{23}$/mol). The cross section is used to to find out the excitation rate (k). It is assumed that the decay intensity of the experiments follows perfect exponential decay form, the lifetime measurement of spontaneous emission can be extracted from the intensity equation.

$$I(t) = I_0 e^{-\frac{t}{\tau}} = I_0 e^{-kt} \tag{12}$$

where I(t) is the varying intensity of emission by time and I_0 is the initial intensity that would be maximum in this decaying situation. The intensity point of which the value of I(t) is $\frac{I_0}{e}$ matches the time when t= τ.

In order to compare a property called quantum yield later, the absorption rate (k_λ) is needed. From the cross section equation [11], the rate is :

$$k_\lambda = \frac{\sigma(\lambda) \cdot I_{exc}}{E} = \frac{A(\lambda) \cdot I_{exc}}{N_a \cdot c \cdot l \cdot E} \tag{13}$$

where E is was the energy difference corresponding to the excitation wavelength 385nm (E=$\frac{hc}{\lambda}$). The excitation intensity (I_{exc}) is equal to the power/pulse (p_p) divided by shot area of the beam.

$$I_{exc} = \frac{p_p}{\pi r_s^2} \tag{14}$$

Here, r_s is the radius of the focused beam on the sample.

$$r_s = 0.61 \frac{\lambda * f}{r} \tag{15}$$

where f is the focal length of converging lens which was 7.5cm and r is radius of the original beam which was 1.2mm. With 386nm of the excitation wavlelength, r_s is computed to be 1.467mm.

2.4 Inner filter effect

When fluorescence is measured in practice, the shape of fluorescence can be somewhat distorted from the absorption spectrum even though mirror symmetry is expected. Here, the inner filter effect can be identified by comparing the absorption and emission spectra. This effect can reduce the intensity of the measured fluorescence [14].

There are two sorts of inner filter effects, which are primary and secondary[15][16]. The primary inner effect is about a situation that the analyte absorbs the incoming excitation light itself which happens all the time. The secondary inner filter effect is about the re-absorption after emitting and this is related to the spectral overlap between absorption and emission. This secondary inner filter effect can be prominent under some circumstances. The factor is the absorbance at emission wavelength.

Before preceding experiments with aggregated molecule, anthracene was used as an example to study secondary inner filter effect in practice. Anthracene is a solid polycyclic aromatic hydrocarbon (PAH) composed of three benzene rings. It is colorless but exhibits a blue fluorescence under ultraviolet (UV) light where λ_{max} = 400–450 nm [17]. In fig [5], when the excitation wavelength for fluorescence is selected at two wavelengths (λ_{ect}= 345nm, 355nm) that one has a high absorbance and the other has a relatively low absorbance; it is much clear with the high absorbing wavelength to check the secondary inner filter effect. As seen in fig [5], the overlapping range between absorption and emission is around 370-380nm and the attenuation is obvious in the emission spectrum of λ_{ect}= 355nm since the measured absorbance is much higher than λ_{ect}= 345nm. The emission intensity at 380nm is reduced when λ_{ect}= 355nm.

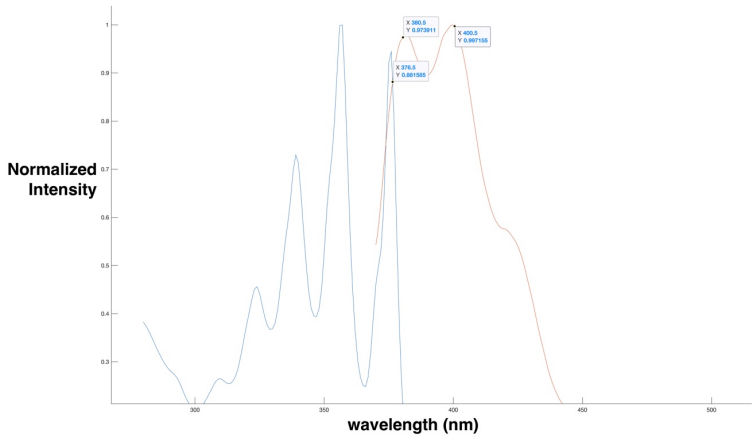

Figure 4: Absorption and emission spectrum of anthracene with excitation wavelength at 345nm

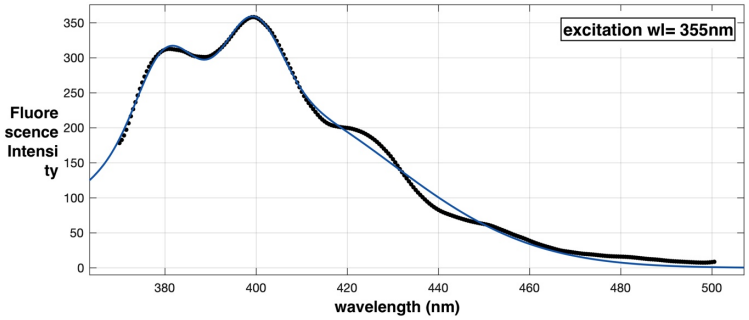

Figure 5: Emission spectrum of anthracene with λ_{ext}= 355nm

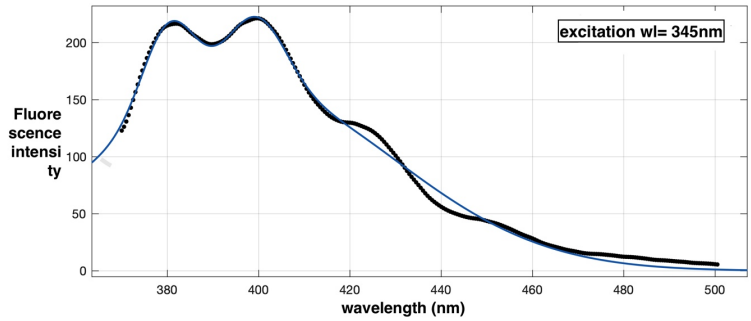

Figure 6: Emission spectrum of anthracene with λ_{ext}= 345nm

Also, this equation (16) explains where the maximum intensity of unaffected emission can locate in the spectrum after correction [16].

$$F_{corr} = F_{obs} * 10^{\frac{A_{ex}+A_{em}}{2}} \tag{16}$$

, where F_{obs} is the maximum intensity of emission, and F_{corr} is the maximum intensity after correcting the inner filter effect. A_{ex} and A_{em} are the absorbance at the excitation wavelength and maximum emission wavelength.

2.5 Quantum yield

In order to compare the fluorescence quantum yield (Φ) of monomers and aggregates, each number of absorbed photons and emitted photons is needed. 'k' denotes the rate of fluorescence (k_{fl}) and non-radiative emission (k_{nr}).

$$\Phi = \frac{k_{fl}}{k_{fl} + k_{nr}} \tag{17}$$

The fluorescence rate of monomer (k_{mfl}) is proportional to the square magnitude of dipole moment of that monomer ($\vec{\mu_m}$).

$$k_{mfl} \propto \vec{\mu_m}^2 \tag{18}$$

So, in aggregated molecules, N is the number of molecules over which excitation is delocalized. Then the transition dipole of N molecules can be written as:

$$\vec{\mu_N} = \frac{1}{\sqrt{N}} N \vec{\mu_m} = \sqrt{N} \vec{\mu_m} \tag{19}$$

$$\vec{\mu_m}^2 = (\frac{\mu_N}{\sqrt{N}})^2 = \frac{{\mu_N}^2}{N} \tag{20}$$

The fluorescence rate of aggregates can be also written as

$$k_{Nfl} \propto \vec{\mu_N}^2 \tag{21}$$

$${\mu_N}^2 \propto N * k_{mfl} = k_{Nfl} \tag{22}$$

So the delocalization of excitons in aggregates (N) can be extracted by dividing k_{Nfl} by k_{mfl}.
k_λ is computed from the Beer-lambert propagation, but given that the streak camera measurement records photons only from one direction, k_{fl}, which accounts for all emitted photons, cannot be achieved from a limited angle. Instead, quantum yield from limited angle (Φ_a) can be defined as:

$$\Phi_a = \frac{N_{emitted photons}}{N_{absorbed photons}} \tag{23}$$

Φ_a will be measured with the given setup and the local quantum yield will be defined by multiplying collection efficiency of the setup (Φ_{col}) as:

$$\Phi_a = \Phi \cdot \Phi_{col} \tag{24}$$

3 Experimental Setup

3.1 Absorption

The spectrophotometer used in the experiments was UV 2600/2700i Shimadzu. The optical layout is given in fig[7]. The wavelength range was set up from 350nm to 500nm. The beam first goes through an reference path which is placed at the top. Then, the beam is reflected and penetrates the sample path that can be embedded with the cuvette. Either area of $1*1cm^2$ or $1*0.1cm^2$ sized cuvette can fit into the sample path. Two detectors compare the reference path to the sample path. The logarithm of the intensity tells how much the material has absorbed the light in varying wavelengths.
Also, before proceeding measurements, absorbance of reference path should be measured in order to achieve accuracy of latter experiments, which is called the baseline absorption measurement. The spectrum of the baseline is automatically subtracted from the latter results.

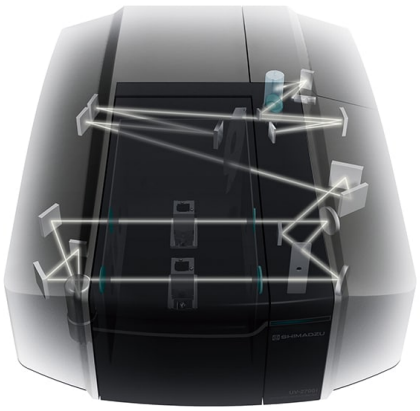

Figure 7: Absorption spectrophotometer configuration

3.2 Fluorescence

3.2.1 Fluorescence measurement by wavelength

The first set of fluorescence measurements was carried out at a perpendicular geometry as seen in fig[8]. The excitation wavelengths of the beam were chosen from the absorbance spectrum. The beam was shot directly onto the solution, which was all contained in $1*1cm^2$ cuvette. The detector catches a ray of the emitting light at the perpendicular angle next to the cuvette. This setup measures the emission only by wavelength.
The emitting ray also goes through the same decaying procedure in the overlapped area [18]. In the used fluorescence spectrophotometer, the ray is placed perpendicular to the direction of the detector. So, the attenuation which follows Beer-Lambert law happens twice to the excitation light and to the emitting light from the center.

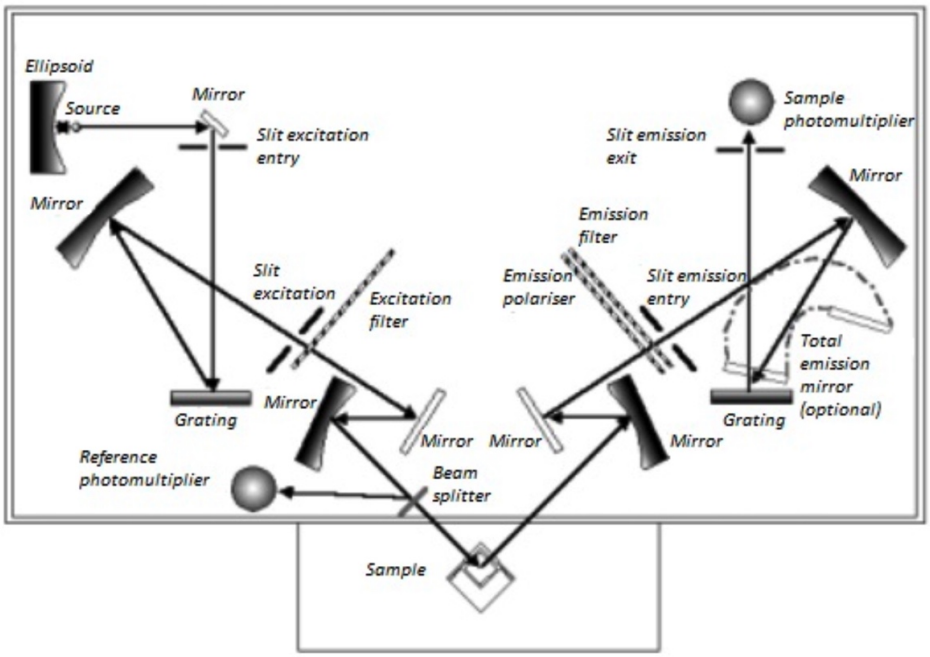

Figure 8: 1D fluorescence optical layout

3.2.2 Streak camera

The second set of fluorescence measurements were done with a streak camera. The major principle of this camera is similar to the previous fluorescence machine, but it instead counts photons by time and wavelength [19]. The primary purpose of using this streak camera is to determine the lifetime of fluorescence decay. The camera measures the emission wavelength in nm, the time in picoseconds.

The working principle of a streak camera is illustrated in fig [9]. The light pulse is directed to the streak tube's photocathode, which converts photons into electrons [19]. The photoelectrons are accelerated by the accelerating mesh, then pass via a pair of sweeping electrodes, multiply in a microchannel plate (MCP), and finally strike the streak tube's phosphor screen, where they are reconverted into an optical picture, so-called streak image. A voltage ramp is supplied to the photoelectrons as they pass through the deflection electrodes, sweeping the electrons from top to bottom. Electrons leaving the photocathode at an earlier period arrive towards the top of the phosphor screen, whereas electrons leaving the photocathode later come near the bottom of the screen. So, the photoelectrons left the cell at a specific moment and then the vertical location of the photoelectrons in the streak image can be used to identify when they exited the photocathode. Because a spectrograph was employed to focus the spectrum onto the photocathode, the horizontal location of the photoelectron is dependent on the wavelength.

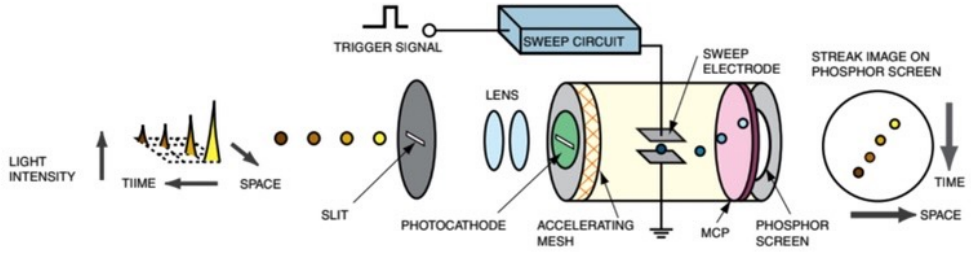

Figure 9: Streak camera optical layout

3.3 Programmable heat tub

The samples go through an heating process, and the purpose of heating and cooling is to find out if the molecules aggregated better and if there is a change in absorption and emission spectrum.
The heat tub has different modes with adjustable heating and cooling cycle. There are two sets of modes which were used for controlling temperature and cooling time. The first set of heat tub experiments was proceeded by setting MCH from 84°C- 91°C for 30, 60,and 120 minutes after reaching a stable temperature. The boiling temperature of MCH is 101°C, so the heating procedure was carried out carefully so that the concentration of liquid did not change exceedingly during the experiment. The stable temperatures that the solvents reached were 84°C for 30 min, 86°C for 60 min and 91°C for 120 min.

4 Results

The result consists of three parts: The first set of experiments starts with measuring the absorption and fluorescence spectrum of CBT dissolved in THF and MCH with three different concentrations at room temperature. The key is to identify optical properties of self-assemblies visualized on the absorption and emission spectrum in different concentrations. The second set is about measuring the spectra after heating the same samples for a different amount of time. By establishing different exposure periods, it is possible to see if the heat influences aggregation and the fluorescence spectrum. The last experiment was proceeded with a streak camera to analyze fluorescence by time and wavelength. The data of the highest concentrated solutions with THF and MCH was analyzed from two perspectives: repetition rate and power per pulse. With the fluorescence decay, the delocalization length of exciton and some properties were calculated.

4.1 Absorption and emission spectrum

The absorption spectrum gives a lot of information about the molecular structure.
1. Shape wise: Aggregation can be assessed by how sharp the peak is. There are two properties to judge aggregation level: peak intensity ratio and linewidth. The peak intensity ratio is a height ratio between two high intensities. Linewidth was achieved from the Gaussian fitting. Two mixtures of CBT molecules showed different absorption spectrum shapes. Numerical comparison will be given later in the Discussion, but here it is possible to read that MCH solution has a higher peak intensity ratio and a smaller linewidth as seen in fig [10]. The highest peak of the THF solution's absorption spectrum is less sharp than one from the MCH solution's spectrum. So, the shape conveys information that the monomer is formed when CBT is dissolved in THF, and the MCH solution functions as J-aggregate.

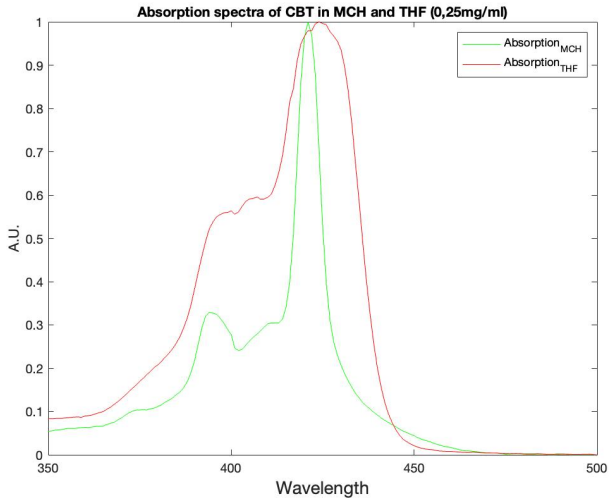

Figure 10: Absorption spectra of CBT in THF and MCH (0.25mg/ml)

2. Choosing excitation wavelengths: Roughly three Gaussians were assumed to compose the absorption spectrum in fig [10], and each Gaussian from eq (1) was made via fitting in the Matlab. Table [1] is one example from MCH solution spectrum. The rest of the Gaussian distribution coefficients is shown in table [4] and [5] in the appendix. Each coefficient 'E' can be converted to wavelength scale and that wavelength was picked as the excitation wavelength for following fluorescence experiments since fluorescence depends on the absorbance.

0.25g/L	Coefficients (error range)
I1	2.309 (2.274, 2.345)
I2	0.8522 (0.8347, 0.8698)
I3	0.3726 (0.3349, 0.4102)
E1(eV)	2.944 (2.944, 2.944)
E2(eV)	3.031 (3.026, 3.036)
E3(eV)	3.147 (3.145, 3.15)
w1(eV)	0.02853 (0.02799, 0.02908)
w2(eV)	0.2071 (0.2017, 0.2126)
w3(eV)	0.03423 (0.02972, 0.03875)

Table 1: Coefficients of gaussians of MCH solution

Same procedures were carried out with three different concentrated samples of THF and MCH solvents. Three wavelengths from three Gaussian distributions were chosen for the excitation wavelengths for fluorescence experiments. In table [2], samples labelled with 1 and 2 are dissolved in MCH and THF respectively. 'a' samples have the highest concentrations with 0.25mg/ml, and 'b' have 0.025mg/ml, and 'c' have 0.0025mg/ml by alphabetical orders.

MCH	1a (0.25mg/mL)	1b (0.025mg/mL)	1c (0.0025mg/mL)
wavelength-1	421	421	425
wavelength-2	409	410	400
wavelength-3	395	378	218-
THF	**2a (0.25mg/mL)**	**2b (0.025mg/mL)**	**2c (0.0025mg/mL)**
wavelength-1	425	430	420
wavelength-2	402	420	411
wavelength-3	378	403	401

Table 2: Three peak wavelengths extracted from fitted absorption spectra

From fig [11], the absorption spectrum of THF shows non-aggregated material's spectrum. All the absorption spectra's peaks seem less sharp than the previous set. For 2a, an overlapped area is formed around 441nm. There are emission peaks at 467nm, 451nm, 450nm each.

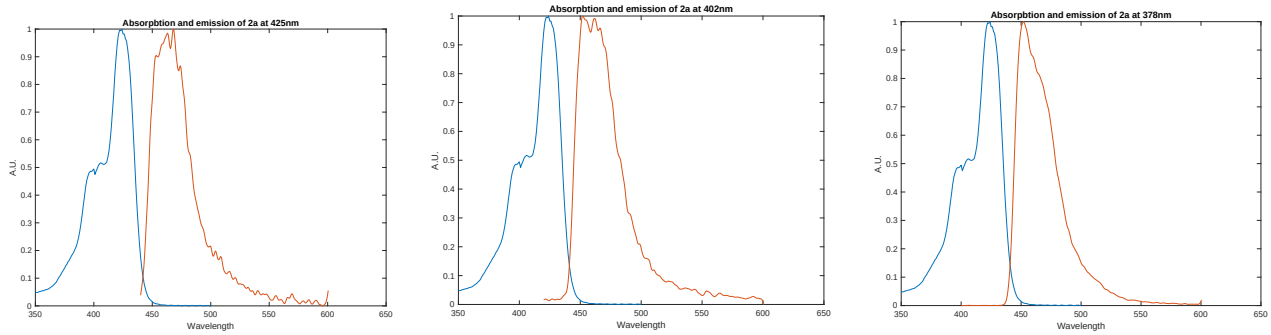

(a) c_m= 0.25mg/ml (2a) excited at λ_{exc}= 425nm

(b) c_m= 0.25mg/ml (2a) excited at λ_{exc}= 402nm

(c) c_m= 0.25mg/ml (2a) excited at λ_{exc}= 378nm

Figure 11: THF solution with 0.25mg/ml concentration (2a) at three different excitation wavelengths (wavelength scale:nm)

For 2b, the shape of fluorescence looks like a mirrored image of the absorption graph. The overlapped area is formed around 438nm. If we look at fig [12], they all look quite mirrored. However, when we compare fig [11a] and [12a], the excitation wavelengths are nearly the same though, the fluorescence with higher concentration reduces at $\lambda = 447nm$. Some parts of the 2a emission disappeared due to the reabsorption which is the secondary inner filter effect.

By applying eq (16) to fig [12b], the corrected maximum intensity of emission can be calculated. Assuming that the cuvette was placed in the exact center of the photospectrometer, F_{corr} becomes 49.9 with the values: A_{ex} = 3.1574 (λ_{exc}= 420nm), A_{em}= 0.2392 ($\lambda_{em.max}$= 447nm), F_{obs}= 16.88. So, reabsorbance was identified and the correction of the secondary inner filter effect was made.

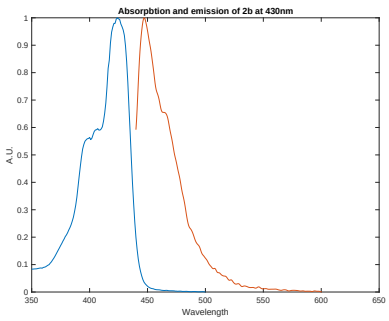

(a) c_m= 0.025mg/ml (2b) excited at λ_{exc}= 430nm

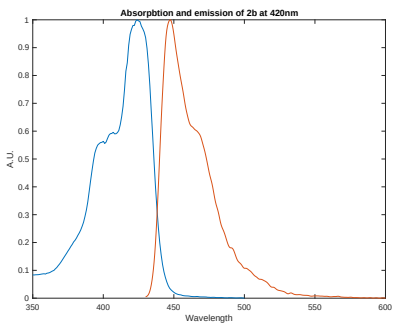

(b) c_m= 0.025mg/ml (2b) excited at λ_{exc}= 420nm

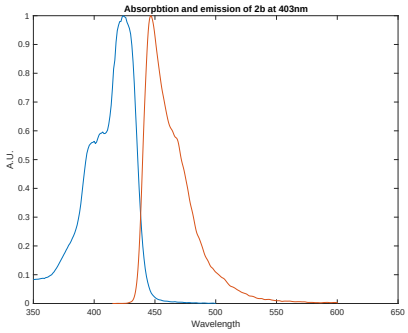

(c) c_m= 0.025mg/ml (2b) excited at λ_{exc}= 403nm

Figure 12: THF solution with 0.025mg/ml concentration (2b) at three different excitation wavelengths (wavelength scale:nm)

Data of 2c follows previous results of fig [12]. The shape and the position of fluorescence is almost identical with fig [12] and the absorption spectrum had a significant noise.
Some optical properties were found by merging the absorption and emission spectrum after normalization in fig [13]. The red fluorescence spectra in fig [13a] and fig [13b] appear to have one slim Gaussian, but the mean value is not at the center, and it is more than one Gaussian indeed. The spectrum is asymmetric, and it only looks so smooth because the re-absorption occurs actively in the range between λ = 420nm - 470nm. Even though the molecules do emit energy in the range, the full emission is not shown in the graph since the absorption is quite dominant in the same range and it seems like emission is not present on the spectrum. So, it is hard to detect that Stoke shift is hardly observed in J-aggregates [20].
Moreover, regardless of the excitation wavelengths, the emission peaks are at 471nm for all emission spectra. That is because there is an overlapped area around 446nm which absorption and emission occur simultaneously, and the measured emission increases as the re-absorption decreases . 1b sample has the middle concentration, and it is considered still well aggregated by accounting for the absorption graph. Inner filter effects are still observable, and the location of peaks can also be explained as before.
With fig [13], it also indicates that the concentration change affects aggregation. The peak intensity ratio between two high peaks of absorption spectrum increases as the concentration becomes lower. That means the relative intensity depends on concentration and the interaction of CBT molecules is related to this property as well.

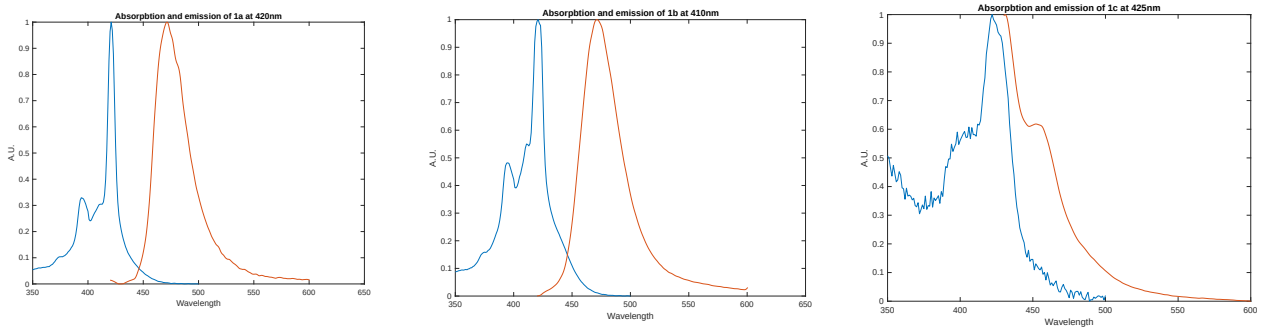

(a) c_m= 0.25mg/ml (1a) excited at λ_{exc}= 421nm

(b) c_m= 0.025mg/ml (1b) excited at λ_{exc}= 421nm

(c) c_m= 0.0025mg/ml (1c) excited at λ_{exc}= 425nm

Figure 13: Absorption and emission spectra of MCH solution at the highest excitation wavelengths (wavelength scale:nm)

Fig [14] with the poorest concentrated solutions, the molecules were excited at a relatively wide range of excitation wavelengths $\lambda_{exc} = 218 - 425nm$. Lots of noise are recorded in the measurements because the closer it gets to the UV spectrum, the more absorption happens. Overlapped areas are formed around 430nm for all three, but the fluorescence spectra have a quite fluctuating shape.

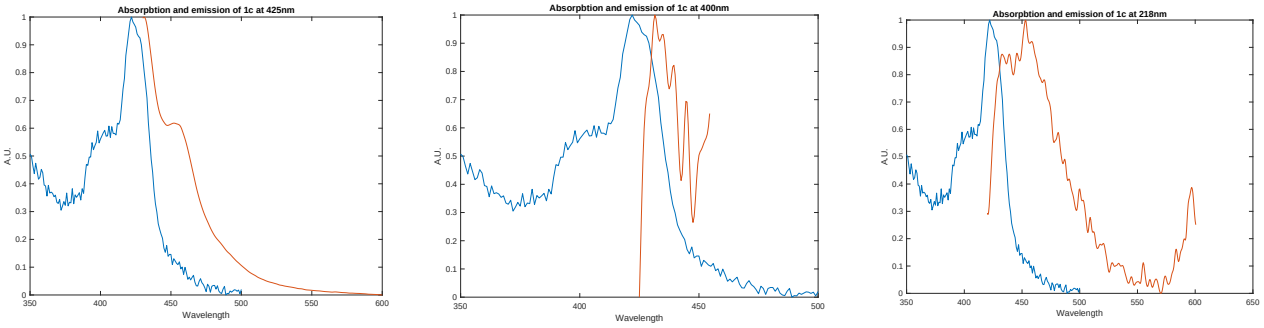

(a) $\lambda_{exc} = 425nm$

(b) $\lambda_{exc} = 400nm$

(c) $\lambda_{exc} = 218nm$

Figure 14: MCH solution with c_m= 0.0025mg/ml (1c) at three different excitation wavelengths (wavelength scale:nm)

So, from three different concentrations, we could assume that the wavelength where absorption and emission occur simultaneously depends on the aggregation and the wavelength shift. Under various excitation energies, it happens to occupy the same overlapped area, whereas intensity is clearly different. In most graphs, there is no significant overlap, and the shape looks almost identical. However, clear interpretations about fig [14b] and [14c] can be hardly made since the fluorescence spectrum had too much noise.

4.2 Absorption and emission spectrum after heat exposure

To see if there is any effect in further aggregation, two high concentrated MCH samples were heated for 30, 60, 120 minutes at a high temperature, where the aiming temperature of heat tub was 95°C and the reached temperature was approximately 86°C. The derived data are categorized by concentrations and heating time.

4.2.1 Comparing data under same exposure time

Graphs in fig [15] are normalized to see the wavelengths shift among different concentrations. From those graphs, it seems that the wavelengths of maximum intensity of high concentrated solvents tend to be longer than low concentrated ones, and the overall absorption and emission spectrum had blue shifted when the heating time got longer.

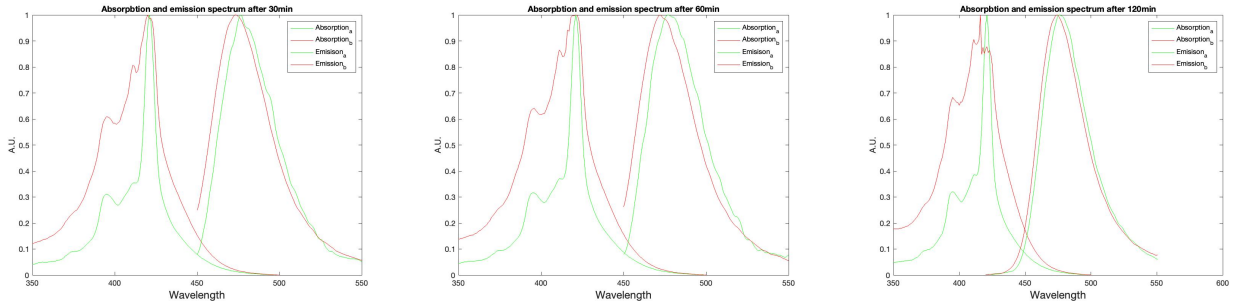

(a) 30 minutes exposure (b) 60 minutes exposure (c) 120 minutes exposure

Figure 15: Two high concentrated MCH solutions under different heating time (green spectra:c_m= 0.25mg/ml, red spectra: c_m= 0.025mg/ml)(wavelength scale:nm)

4.2.2 Absorption graphs

In the sufficiently aggregated samples of fig [16a] and [16b], the absorption spectra look almost identical and the characteristic did not change after the temperature exposure. Absorbance slightly increased due to additional thermal exposure when the concentration is low.
Since all the absorption data is at one place, aggregation of each concentration under different heating time can be estimated through fitting the sharpest peaks. From two absorption graphs of fig [16a] and [16b], the data match with each other, therefore the linewidths of peaks share the similar values.

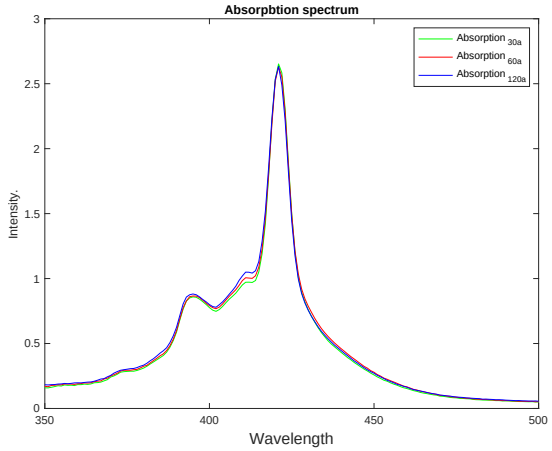

(a) c_m= 0.25mg/ml

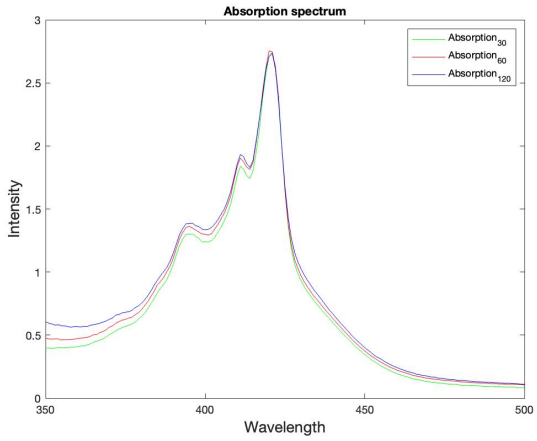

(b) c_m= 0.025mg/ml

Figure 16: Absorption spectrum of MCH in different exposure time (wavelength scale:nm)

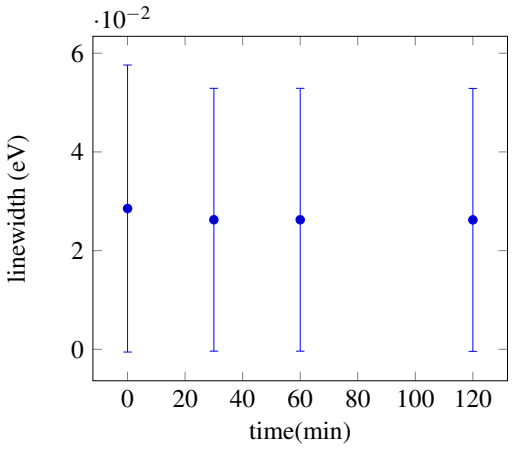

(a) Aggregation change of 1a

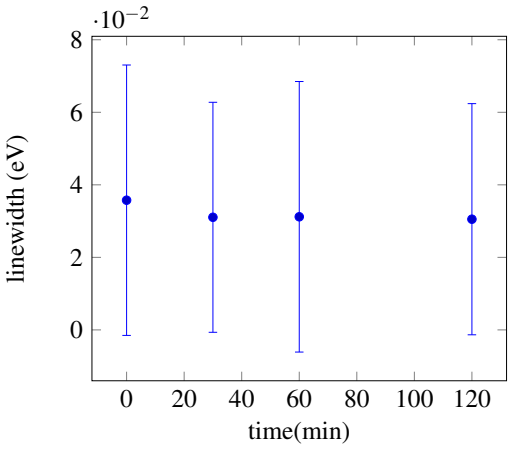

(b) Aggregation change of 1b

Figure 17: Aggregation distribution by time

With the medium concentrated sample, intensities of emission were compared with the absorption as well. There is a phenomena discovered in putting emission together, which will be discussed in depth in the next section.

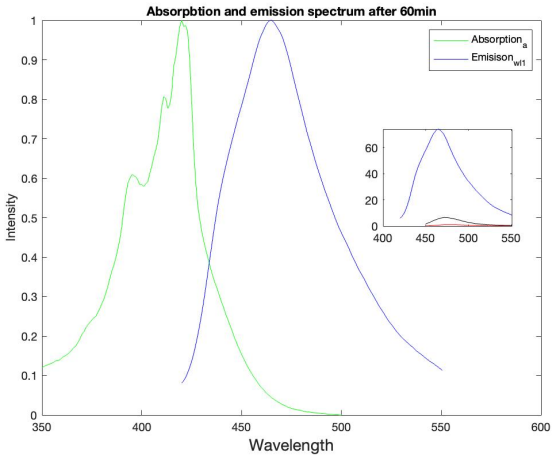

Figure 18: Absorption and all emissions of MCH sample (c_m= 0.025mg/ml)(wavelength scale:nm)

4.2.3 Fluorescence graphs

The excitation wavelength was kept on 420nm for 30 min and 60 min experiments, but on 400nm for 120 min experiment. In fig [16a], the absorbance at 420nm is around 2.5 times higher than that of 400nm. In fig [16b], the absorbance at λ_{exc}= 420nm is almost 2 times higher than that of 400nm. These mean that the emission intensities are also supposed to be higher at 420nm, but there is an odd phenomenon seen in the fig [19a] and [19b]. It seems that the fluorescence intensity largely increased after thermal exposure longer than an hour when the molecules are sufficiently aggregated.

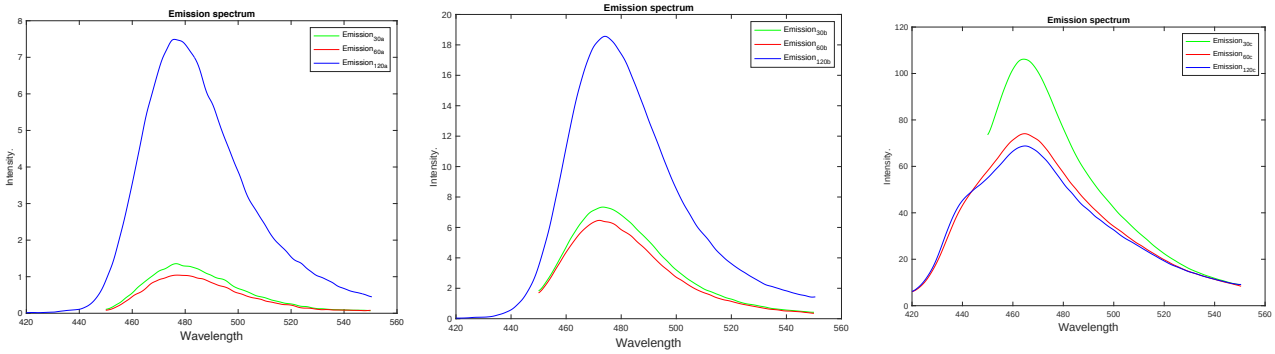

(a) 1a (b) 1b (c) 1c

Figure 19: Emission spectrum of MCH samples in different exposure time (wavelength scale:nm)

In the section 4.1, there were 18 fluorescence spectra produced from 6 absorption spectra. While fitting absorption spectra through the Matlab, three Gaussians were thought to be an adequate number to have a close estimate since the goal of the fitting is to determine properties like the linewidth and the peak ratio. Sometimes, an inconsistently increasing part was excluded from the fitting when three distributions are used. However, in the second heating experiment, there were 5 or 6 distributions used for higher accuracy. Since the linewidth of one big peak is the crucial property to compare

aggregation, and the absorption spectra of MCH showed a high matching probability apart from the poorest concentration measurement, observation of minute change was necessary.

Also, a problem that happened in the second experiment was that the concentration of samples changed while heating them for the exposure time. After 120 minutes of heating, 1b samples were half evaporated, so there were new MCH substituted for reheating.

4.3 Spectral resolved lifetime measurement

In order to measure the photon number from one direction, the streak camera was used this time. The result shows each photon count in different time intervals. The data describe two-dimensional qualities, so by integrating the time of the wavelength, the intensity can be explained by the other non-integrated dimension [21]. By selecting a particular wavelength zone on the x-axis, the line explains a fluorescence decay with the time versus intensity graph. To find out the lifetime of this molecule's decay, the point where it is $\frac{I_{max}}{e}$ should be found, and the time gap between the I_{max} and $\frac{I_{max}}{e}$ was extracted as the lifetime. On the other hand, the previous one-dimensional emission graph with the wavelength and the intensity can be derived by integrating a certain range of time, and this can look the same as the previous fluorescence method after the sum of the entire time.

For every experiment, the power and the repetition rate were varied. The repetition rate is equal to 1.9Mhz/division. This example in fig [20] was carried out with the highest concentrated samples with λ_{exc}= 385nm when the repetition rate is 95kHz and the power is 61μW.

As seen in fig [20], the x-axis and the y-axis of the graph, respectively, indicate the emission wavelength (nm) and time (ps). Each dimension makes a different result after integrating the other factor. The photon distribution in fig [20a] seems to consist of two peaks at λ_{center}= 465nm, λ_{center}= 435nm. So, there were two steps needed to analyze the distribution shape and the decay rate for each peak.

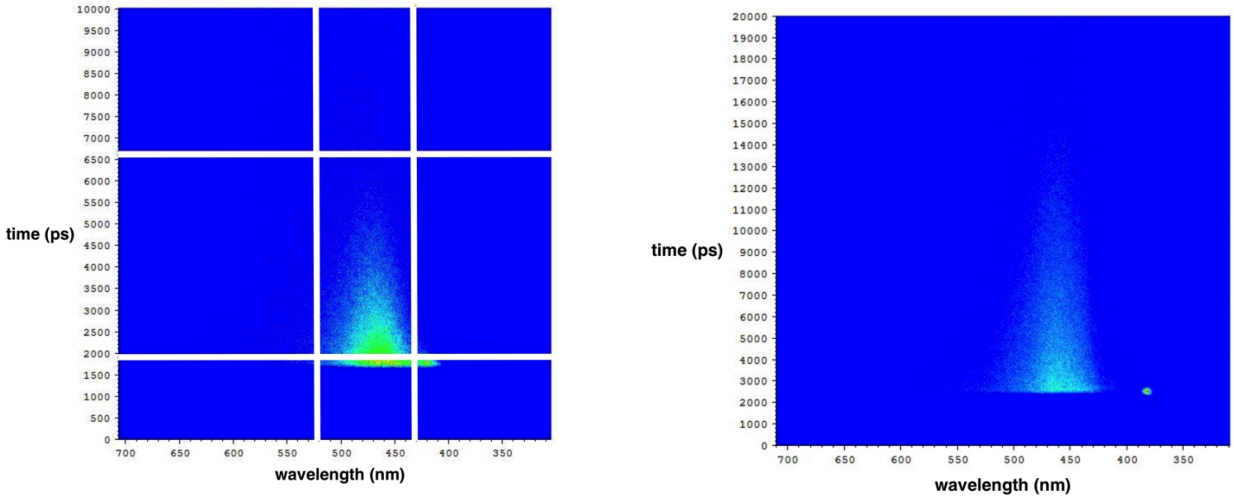

(a) Streak camera image of MCH

(b) Streak camera image of THF

Figure 20: Streak camera images

Fig [21a] was produced by integrating the data points with horizontal lines with a range of 1955-6190 ps. The summation of reaction by each pico-second forms a transient spectrum since there were two peaks in fig [20a]. This is a mere snap in a part of time zone but if these gaussians are entirely stacked up, then the final image would look like other fluorescence spectra in section 4.1 and 4.2.

Fig [21b] is from the integration by wavelength of the big peak, scoping at λ= 447-522nm (in between

the two vertical white line in fig [20a]). The max intensity is a crucial point so as to find the lifetime of this fluorescence decay. The calculation of lifetime is based on the assumption that the experimental functions integrated by wavelength precisely follow the mathematical exponential function. The intensity function has an exponential decrease, and the coordinate t= τ could only be pinpointed from this assumption.

Lifetimes of the highest concentrated sample THF solution was expected by integrating the entire region [fig 20b]. There was only one big photon distribution, so a division of peaks by eyes was impossible. A laser point source is captured by the camera at 386nm.

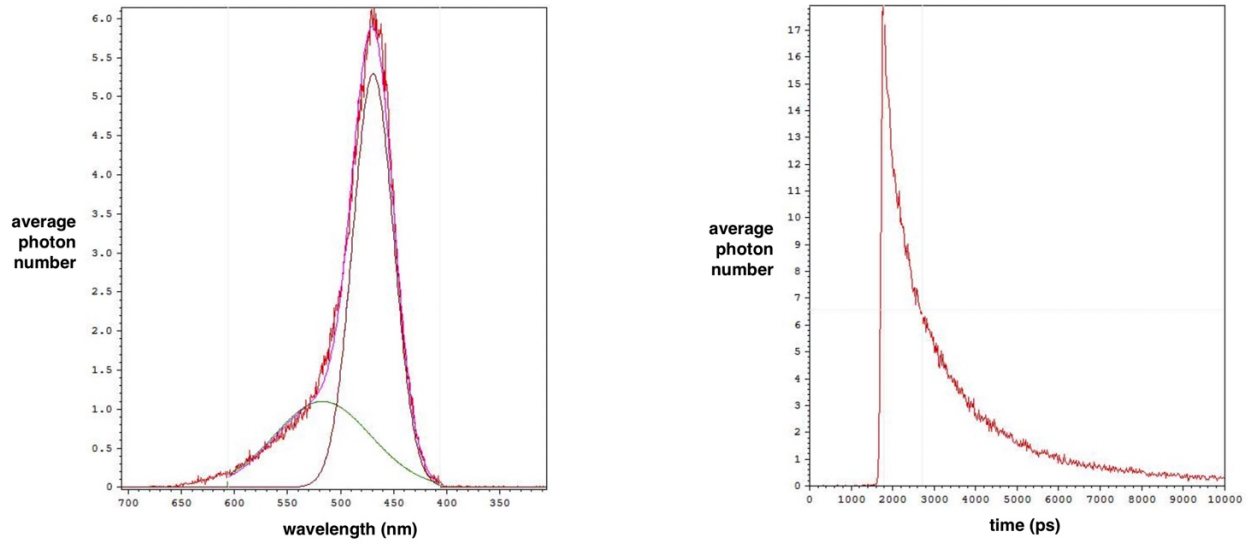

(a) Big peak integrated by time

(b) Big peak integrated by wavelength

Figure 21: Separation integration

In this fig [22], the data points are in three category, which are divided by size of the photon distribution and the sort of analyte. There were six times of measurements with different power and repetition rates. After repeating the lifetime extraction for each photon section (two sections of λ= 447nm +/- in fig [20a] and one section in fig [20b]), eighteen data points of lifetime were made in fig [22]. Green and pink data points are derived from aggregated molecule sample. Black points are made from a one distribution of monomer sample. In overall, monomers tend to have longer lifetimes than aggregated ones in the same condition.

There are four groups overlapped at the right side in the fig [22a] because they share the identical repetition rates as 95kHz. The middle points have 31.6kHz, and the left side has 9.5kHz. As the repetition rates increase, the lifetime of aggregated molecule has slightly increased. For the monomer, the lifetime relatively increased more in the higher repetition rates than aggregated sample when the power per pulse is over 600μW. In the fig [22b], there is a tendency that aggregated molecules show constant lifetimes once its power exceeds 200μW. On the other hand, monomers tend to have longer lifetimes as the power per pulse increased apart from the point of which the repetition rate was recorded at the

lowest in the fig [22a].

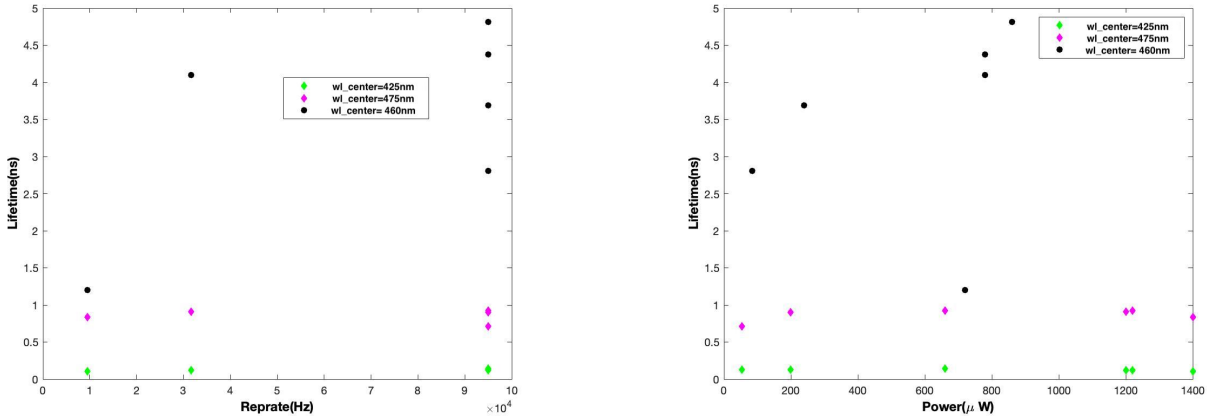

(a) Repetition rate vs lifetime

(b) Power per pulse vs lifetime

Figure 22: Lifetime scattering

So, the next step is to figure out the delocalization length N. In order to know N, the first thing to calculate is the cross section of the beam ($\sigma(\lambda)$). With the equation (11), the cross section was calculated as $2.29 * 10^{-10} m^2$ when the absorbance was recorded as 0.4164 at 385nm of the excitation wavelength. As seen in the previous figures [22], aggregation affects to the shorter lifetime and that leads to yielding higher fluorescence k rate (k_{Nfl}) than monomer's rate (k_{mfl}). In table [3], the partial quantum yield () that is the fluorescence rate divided by each excitation k rate has greater values with aggregated molecules. Also, since N is the ratio between two fluorescence rates of the different molecules, each number of N was created from experiments. The mean value of delocalization length in the exciton is 19.9 monomers. However, there was a strong delocalization up to 40 monomers along the self-assembled nanostructures.

Properties						
file (rep rate)	1 (95kHz)	2 (95kHz)	3(95kHz)	4(95kHz)	5 (31.6kHz)	6 (9.5kHz)
τ (MCH) [10^{-10} s]	1.246	1.097	1.070	1.085	1.082	0.9253
τ (THF)(ns)	4.810	3.693	2.810	4.377	4.094	1.204
p_p (MCH)[W]	6.6*10^{-4}	2.0*10^{-4}	5.4*10^{-5}	1.2*10^{-3}	1.2*10^{-3}	1.4*10^{-3}
p_p (THF)[W]	8.6*10^{-4}	2.4*10^{-4}	8.4*10^{-5}	7.8*10^{-4}	7.8*10^{-4}	7.2*10^{-4}
k_λ (MCH)[10^{13}]	4.335	1.313	0.354	8.013	7.882	9.196
k_λ (THF)[10^{13}]	5.649	1.576	0.551	5.123	5.123	4.729
k_{Nfl} (MCH)[10^9]	8.024	9.108	9.339	9.209	9.233	10.807
k_{mfl} (THF)[10^8]	2.079	2.707	3.558	2.284	2.442	8.305
Φ_a (MCH)[10^{-4}]	1.85	6.93	26.32	1.15	1.17	1.17
Φ_a (THF)[10^{-6}]	3.68	17.17	64.49	4.45	4.76	17.56
N	38.597	33.638	26.242	40.312	37.803	13.011

Table 3: Properties needed for partial quatum yield and N

5 Discussion

5.1 Absorption and emission spectrum

Section 4.1 mainly discusses how concentration change of solvent affects aggregation level. The degree of J-aggregation can be judged by comparing the highest peak in the absorption spectrum. That well aggregated molecules show a sharper peak can be proved by checking the energy scheme of J aggregate in section 2.2.3. Two properties would be used as criteria to compare the sharpness: the linewidth and the peak intensity ratio.

First, as the representative example shown in fig [10], the linewidth measured from the highest peak in the monomer spectrum is 0.07617 ($\pm$ 0.002) eV. But, the linewidth measured from the highest peak in MCH solution was found to be 0.02853 ($\pm$ 0.005) eV, which is 2.67 times more narrow than monomer.

So, the first set of experiment is mainly about that there is a change in aggregation level by concentration (fig [13]). The middle concentrated MCH solution has a clear reduction in linewidth and height ratio compared to the most concentrated solution. Its linewidth records as 0.03576 ($\pm$ 0.0151) eV. This value is 1.25 times larger than the linewidth of the most concentrated one. Roughly this could still perform as self-assembly. However, the least concentrated solution has a linewidth measured as 0.08327 ($\pm$ 0.031) eV, leading to a 2.92 times wider peak than the most concentrated solution. Even if the CBT core is dissolved in MCH, the width of the peak is almost as wide as the spectrum of the most concentrated solution of THF. Therefore, the CBT molecules do not assemble in this 0.0025mg/ml concentration and would function as a monomer.

Next, the ratio between two highest peak intensities is computed for comparison. Selecting intensities (I) from two high peaks, and $\frac{I_1}{I_2}$ becomes the peak intensity ratio. In the absorption spectra (fig [10]), the ratio from the CBT spectrum in MCH records 2.71, whereas the ratio from THF solution records 0.93. The ratio of self-assembly is 2.91 times higher than that of monomers.

Moreover, from the fig [10], vibrational energy (hv) of the first excited state could be calculated. Again from the Gaussian distribution fitting, the energy difference of three mean values of distribution represent those vibrational energy. The most concentrated MCH solution yields 0.116 eV and 0.087 eV, the middle concentrated solution yields 0.256 eV and 0.078 eV,the least concentrated solution yields 0.258 eV and 0.178 eV. With the same process, The most concentrated THF solution has 0.196 eV and 0.169 eV. 0.123 eV and 0.07eV for the middle concentrated THF solution. 0.078 eV and 0.062 eV for the least concentrated THF solution. More numbers of vibrational energy could be found accurately if a larger number of Gaussian is used for fitting.

About fig [11] and [12], there seems to be a wavelength shift in the fluorescence spectra. The absorption peak of fig [11] has corresponding energy at 2.914 ($\pm$ 0.003) eV and fig [12] has at 2.882 ($\pm$ 0.004) eV. However, only spectra in fig [12] show a well-mirrored shape between the absorption and fluorescence spectra. This might imply that the corresponding energy of peak intensity of fluores-

cence is rather closer to that of absorption spectrum, and the range close to high absorption is offset due to the secondary inner filter effect.

5.2 Heat treatment

In section [4.2], heat exposure was the key factor in assemblies. Fig [17] implies that the temperature does not have an impact on absorption of aggregated molecules and it might help a little to aggregate better in the lowest concentration seeing that the linewidth increased after 120 minutes possibly due to formationa of assemblies. But for fluorescence, there was an effect of heating to the intensity. As explained in the section [4.2.3], even though the absorbance of 1a sample at 420nm was recorded 2.5 times higher than that of 400nm and the absorbance of 1b sample at 420nm hit 2 times higher than that of 400nm, the order of fluorescence intensity has reversed after 120 minutes of heating in the fig [19a] and [19b]. The fluorescence increased due to the heating treatment and this result might affect the quantum efficiency. Still, the reabsorption is present in this set of measurement again so it is hard to conclude that the quantum yield can definitely increase, but it is likely to increase.

5.3 Spectral resolved lifetime measurement

In section [4.3], fig [20] analysis contains lifetime data as factors of repetition rate and power. Lifetimes of MCH solutions stayed nearly constant the lifetimes with variant power and repetition rate. Since k rates of fluorescence are the inverse number of each lifetime, having no significant change in k rates under different circumstances means no annihilation in this molecule because the excitons do not interact much with near excitons either that the excitons are not mobile enough.

Next, the delocalization number of the exciton (coherence length) is calculated in table [2], ranging from 13 to 40. Ranging up to 40 implies that this aggregate had an active delocalization with that number of monomers. Also, in terms of power and repetition rate, the delocalization number increases when the power becomes stronger, but it is likely to converge around 40. Since there is no annihilation in this system, this converged number would be the maximum delocalization number in this case.

Compared to previous research under different circumstances [22], the delocalization size at low temperatures can enhance up to 50-70 monomers with the prototypical aggregates of the synthetic dye molecule pseudo-isocyanine (PIC). With the disorder strength of $180cm^{-1}$, almost a complete delocalization was achieved by yielding a value of the participation number inside the exciton band that was whole 14,652 molecules in the exciton wave functions.

6 Conclusion

Self-assembly of organic nanofibers have high potentials to improve the efficiency of light harvesting system. This research was mainly focused on optimizing self assembly by experimenting J-aggregate in different situations.

Fist two parts of experiments is about observing aggregation changes under concentrations and heat exposure. Extracting the peak ratio and the linewidth of absorption spectra enabled to compare aggregation numerically. Especially after exposing aggregated sample to 91°C degree for 120 minutes, fluorescence clearly increased even thought the absorbance of the excitation wavelength was lower. Therefore, heat treatment enhanced quantum efficiency due to the increased fluorescence.

The goal of final set was to find out the delocalization length in the exciton and whether it is annihilated in different inputs. J-aggregate would lead to achieving direct energy transport with high quantum efficiency. The tested combination (CBT in MCH) showed no annihilation during decay process. The delocalization length reached up to 40 at room temperature. It is possible to increase the number by adjusting the experiment situation such as temperature. Also, H-aggregate could yield different results due to positive dipole coupling and contribute differently to the coherent transport.

Bibliography

[1] A. Crawls, "Photosynthesis," 8 2000.

[2] F. Fassioli, R. Dinshaw, P. C. Arpin, and G. D. Scholes, "Photosynthetic light harvesting: excitons and coherence," *Journal of The Royal Society Interface*, vol. 11, no. 92, p. 20130901, 2014.

[3] Z. Shahan, "Sunpower panels awarded guinness world record," 6 2011.

[4] F. Institute, "Fraunhofer ise-annual report 2018/19," 12 2019.

[5] D. L. Pulfrey, *Photovoltaic power generation*. 1978.

[6] "Organic solar cell," Aug 2021.

[7] T. Brixner, R. Hildner, J. Köhler, C. Lambert, and F. Würthner, "Exciton transport in molecular aggregates – from natural antennas to synthetic chromophore systems," 8 2017.

[8] J. K. Peter William Atkins, Julio De Paula, *Physical Chemistry*, vol. 11. Oxford University Press,, tenth ed.

[9] K. M. B. Stephen Blundell, Stephen J. Blundell, *Concepts in Thermal Physics*. Oxford University Press, second ed., 2006.

[10] J. McEwe, "Jablonski diagram," aug 2020.

[11] A. I. B. W. M. K. N. H. J. K. H.-W. S. . R. H. Andreas T. Haedler, Klaus Kreger, "Long-range energy transport in single supramolecular nanofibres at room temperature," *Nature*, vol. 523, p. 196–199, july 2015.

[12] J. K. C. L. F. W. Tobias Brixner, Richard Hildner, "Exciton transport in molecular aggregates – from natural antennas to synthetic chromophore systems," *Advanced Energy Materials*, vol. 7, aug 2017.

[13] J. Clark, "The beer lambert law," aug 2020.

[14] H. scientific insititute, "How inner-filter effects (ife) can affect your fluorescence measurements: A case study - colloidal inp quantum dots," jan 2019.

[15] J. R. Lakowicz, *Principles of Fluorescence Spectroscopy*. Springer, third ed., sep 1983.

[16] J.-H. W. . Shuai Chen 1, Yong-Liang Yu 2, "Inner filter effect-based fluorescent sensing systems," *Anal Chim Acta*, pp. 999:13–26, jan 2018.

[17] P. Rao, "Anthracene," in *Encyclopedia of Toxicology (Third Edition)* (P. Wexler, ed.), pp. 260–261, Oxford: Academic Press, third edition ed., 2014.

[18] A. M. SurajKumar Panigrahi, "Inner filter effect in fluorescence spectroscopy: As a problem and as a solution," *Journal of Photochemistry and Photobiology C: Photochemistry Reviews*, vol. 41, dec 2019.

[19] AG biomolekular photonik, *Streak camera*, 2004.

[20] M. Murata, T. Araki, and H. Nakahara, "Study on j-aggregate formation of a long-chain merocyanine in the mixed lb films and their optical behavior," in *Proceedings of the International Conference on Colloid and Surface Science* (Y. Iwasawa, N. Oyama, and H. Kunieda, eds.), vol. 132 of *Studies in Surface Science and Catalysis*, pp. 561–564, Elsevier, 2001.

[21] H. Ku, *Streak camera*. AG biomolekular photonik, aug 2021.

[22] T. L. C. J. Anna S. Bondarenko and J. Knoester, *Exciton localization in tubular molecular aggregates: size effects and optical response*. PhD thesis, University of Groningen, Zernike Institute for Advanced Materials, Nijenborgh 4, 9747 AG Groningen, The Netherlands, mar 2020.

Appendices

A Additional data

	1a (0.25mg/mL)	1b (0.025mg/mL)	1c (0.0025mg/mL)
I1	2.309 (2.274, 2.345)	1.547 (1.504, 1.59)	0.07433 (0.07246, 0.07621)
I2	0.8522 (0.8347, 0.8698)	1.99 (1.923, 2.057)	0.03132 (0.02976, 0.03288)
I3	0.3726 (0.3349, 0.4102)	0.4576 (0.3809, 0.5342)5	0.155 (-0.4925, 0.8024)
E1(eV)	2.944 (2.944, 2.944)	3.023 (3.018, 3.028)	2.918 (2.915, 2.92)
E2(eV)	3.031 (3.026, 3.036)	2.945 (2.945, 2.946)	3.093 (3.085, 3.1)
E3(eV)	3.147 (3.145, 3.15)	3.279 (3.074, 3.484)	5.687 (-3.086, 14.46)
w1(eV)	0.02853 (0.02799, 0.02908)	0.2249 (0.217, 0.2328)	0.08327 (0.08021, 0.08632)
w2(eV)	0.2071 (0.2017, 0.2126)	0.03576 (0.03425, 0.03728)	0.1036 (0.09325, 0.1139)
w3(eV)	0.03423 (0.02972, 0.03875)	0.03043 (0.02395, 0.03691)	2.208 (-2.728, 7.144)
d	2.312e-14	0.06083 (0.03547, 0.0862)	0.01915 (-0.02142, 0.05973)

Table 4: Coefficients of gaussians of MCH

	2a (0.25mg/mL)	2b(0.025mg/mL)	2c (0.0025mg/mL)
I1	2.474 (2.381, 2.567)	2.236 (2.091, 2.381)	0.02876 (0.02702, 0.03051)
I2	1.178 (0.7946, 1.562)	1.644 (1.472, 1.816)	0.009193 (0.007971, 0.01041)
I3	0.2548 (0.1121, 0.3976)	1.845 (1.823, 1.867)	0.01967 (0.01892, 0.02042)
E1(ev)	2.914 (2.912, 2.917)	2.882 (2.878, 2.886)	2.95 (2.948, 2.952)
E2(ev)	3.083 (3.075, 3.091)	2.952 (2.947, 2.956)	3.012 (3.004, 3.02)
E3(ev)	3.279 (3.074, 3.484)	3.075 (3.071, 3.079)	3.09 (3.081, 3.098)
w1(eV)	0.07617 (0.07409, 0.07824)	0.05087 (0.04809, 0.05366)	0.02759 (0.02544, 0.02974)
w2(eV)	0.1245 (0.1022, 0.1468)	0.04762 (0.04401, 0.05123)	0.03998 (0.0289, 0.05106)
w3(eV)	0.2134 (0.05016, 0.3767)	0.163 (0.1574, 0.1686)	0.2581 (0.2437, 0.2725)
d	6.357e-10	0.1382 (0.1288, 0.1476)	0.0373 (0.03687, 0.03773)

Table 5: Coefficients of gaussians of THF

	30min	60min	120min
I1	1.744 (1.724, 1.764)	1.678 (1.659, 1.697)	1.648 (1.628, 1.669)
I2	0.6913 (0.6734, 0.7091)	0.3283 (0.3107, 0.3459)	0.7199 (0.7016, 0.7381)
I3	0.3182 (0.3003, 0.336)	0.7174 (0.7006, 0.7342)	0.3364 (0.3171, 0.3557)
I4	0.3402 (0.3213, 0.359)	0.3249 (0.3079, 0.3418)	0.3472 (0.3296, 0.3648)
E1(eV)	2.944 (2.944, 2.944)	2.944 (2.944, 2.944)	2.945 (2.945, 2.945)
E2(eV)	2.975 (2.972, 2.978)	3.146 (3.145, 3.148)	2.978 (2.976, 2.981)
E3(eV)	3.125 (3.113, 3.138)	2.974 (2.972, 2.976	3.148 (3.147, 3.15
E4(eV)	3.146 (3.144, 3.147)	3.128 (3.116, 3.14)	3.121 (3.11, 3.132)
w1(eV)	0.02626 (0.02588, 0.02663)	0.02626 (0.0259, 0.02663)	0.02623 (0.02582, 0.02664)
w2(eV)	0.1537 (0.1482, 0.1593)	0.04017 (0.03761, 0.04274)	0.1489 (0.1437, 0.1541)
w3(eV)	0.4466 (0.4298, 0.4634)	0.1561 (0.1511, 0.1612)	0.04041 (0.03765, 0.04316)
w4(eV)	0.04067 (0.03801, 0.04334)	0.4557 (0.4394, 0.472)	0.4501 (0.4341, 0.4661)

Table 6: Coefficient of gaussians of absorption spectrum after heating 1a

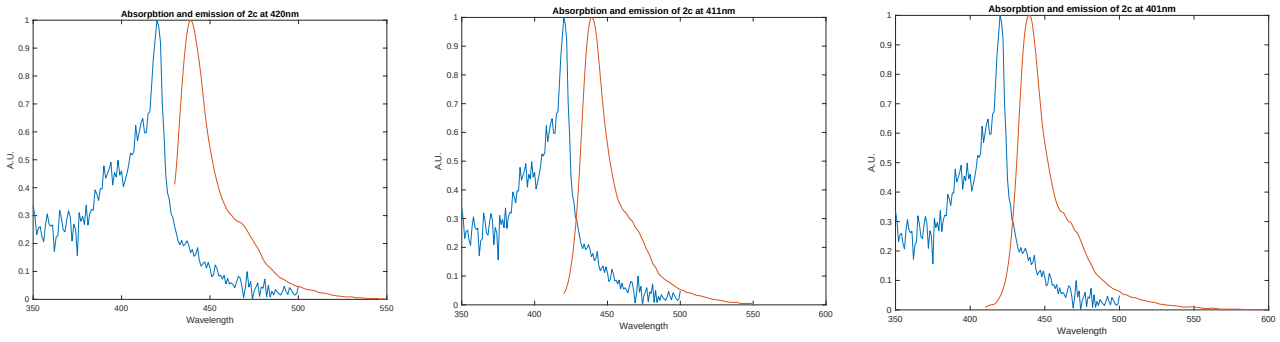

(a) 2c1 (b) 2c2 (c) 2c3

Figure 23: THF solution with c_m= 0.0025mg/ml (2c) at three different excitation wavelengths (scale:nm)

eV	30min	60min	120min
I1	0.1123 (-0.03743, 0.262)	0.05948 0.04516, 0.07381)	1.528 (1.5, 1.556)
I2	0.09969 (0.01377, 0.1856)	0.1465 (-0.04976, 0.3428)	0.1441 (0.05422, 0.234)
I3	0.04165 (0.03395, 0.04935)	0.03385 (0.02744, 0.04026)	0.5189 (0.4909, 0.5469)
I4	0.09622 (0.0726, 0.1198))	0.06597 (0.03808, 0.09386)	0.1531 (0.1257, 0.1804))
I5		0.0334 (0.01946, 0.04734)	1.412 (1.395, 1.43)
E1(eV)	2.817 (2.785, 2.848)	2.763 (2.748, 2.778)	2.947 (2.946, 2.948))
E2(eV)	3.515 (3.502, 3.529)	4.796 (0.9591, 8.634)	2.977 (2.974, 2.981)
E3(eV)	2.494 (2.483, 2.505)	3.467 (3.46, 3.474)	3.014 (3.012, 3.016)
E4(eV)	3.175 (3.011, 3.339))	2.899 (2.889, 2.91)	3.149 (3.146, 3.153)
E5(eV)		3.051 (2.984, 3.118)	3.049 (3.048, 3.051))
w1(eV)	0.2093 (0.1414, 0.2772)	0.03119 (0.03045, 0.03192)	0.03052 (0.02917, 0.03187)
w2(eV)	0.1485 (0.1024, 0.1946)	0.03 (0.02744, 0.03257)	0.01201 (0.005287, 0.01873))
w3(eV)	0.1058 (0.08909, 0.1224)	0.03251 (0.02773, 0.0373)	0.02841 (0.02546, 0.03135))
w4(eV)	0.3545 (-0.1956, 0.9046)	0.2128 (0.2061, 0.2194)	0.02507 (0.01941, 0.03073)
w5(eV)		0.1457 (0.09011, 0.2012)	0.2674 (0.2642, 0.2705)

Table 7: Coefficient of gaussians of absorption spectrum after heating 1b

	30min	60min	120min
I1	0.04306 (0.02254, 0.06358)	0.05973 (0.04265, 0.07682)	0.0507 (0.03756, 0.06383)
I2	0.07874 (-0.02313, 0.1806)	0.17 (-0.2278, 0.5678)	0.07125 (0.05131, 0.09118))
I3	0.05856 (0.03992, 0.07719)	0.03286 (0.0246, 0.04113)	0.1107 (-0.1997, 0.4211)
I4	0.05471 (-1.022, 1.131)	0.06678 (0.03393, 0.09962)	0.1159 (0.1027, 0.1291)
I5	0.05565 (-0.009547, 0.1209)	0.03356 (0.01738, 0.04974)	0.04504 (-0.009408, 0.0995)
E1(eV)	2.915 (2.897, 2.933)	2.763 (2.745, 2.781)	2.763 (2.754, 2.771)
E2(eV)	3.497 (3.441, 3.554)	5.229 (-1.365, 11.82)	2.906 (2.9, 2.913)
E3(eV)	2.777 (2.761, 2.792)	3.471 (3.461, 3.481)	3.072 (2.873, 3.271)
E4(eV)	5.503 (-2.367e+05, 2.367e+05)	2.9 (2.888, 2.912)	3.516 (3.506, 3.525)
E5(eV)	3.069 (2.933, 3.205)	3.053 (2.975, 3.132)	2.538 (1.163, 3.913)
w1(eV)	0.09382 (0.07412, 0.1135)	0.09005 (0.07827, 0.1018)	0.08288 (0.0701, 0.09567)
w2(eV)	0.1462 (0.07562, 0.2167)	2.513 (-1.08, 6.106)	0.08957 (0.07655, 0.1026)
w3(eV)	0.102 (0.0869, 0.1171)	0.08217 (0.06558, 0.09875)	0.3064 (0.03525, 0.5775)
w4(eV)	184.6 (-7.821e+06, 7.821e+06)	0.1009 (0.07014, 0.1316)	0.1759 (0.1522, 0.1995)
w5(eV)	0.2866 (0.05899, 0.5143)	0.145 (0.07853, 0.2115)	0.4958 (-2.673, 3.664)

Table 8: Coefficient of gaussians of absorption spectrum after heating 1c